Mon. Not. R. Astron. Soc. **386,** 2345–2352 (2008) doi:10.1111/j.1365-2966.2008.13221.x

The fossil phase in the life of a galaxy group

Alexander M. von Benda-Beckmann,[1]⋆ Elena D'Onghia,[2]† Stefan Gottlöber,[1] Matthias Hoeft,[3] Arman Khalatyan,[1] Anatoly Klypin[4] and Volker Müller[1]

[1]*Astrophysical Institute Potsdam, An der Sternwarte 16, Germany*
[2]*Institute for Theoretical Physics, University of Zurich, Winterthurerstrasse 190, Switzerland*
[3]*Jacobs University Bremen, Campus Ring 12, Germany*
[4]*Astronomy Department, New Mexico State University, MSC 4500, PO Box 30001, Las Cruces, NM 880003-8001, USA*

Accepted 2008 March 12. Received 2008 February 12; in original form 2007 October 5

ABSTRACT

We investigate the origin and evolution of fossil groups in a concordance ΛCDM cosmological simulation. We consider haloes with masses between 1×10^{13} and $5 \times 10^{13}\, h^{-1}\, \mathrm{M}_{\odot}$, and study the physical mechanisms that lead to the formation of the large gap in magnitude between the brightest and the second most bright group member, which is typical for these fossil systems. Fossil groups are found to have high dark matter concentrations, which we can relate to their early formation time. The large magnitude gaps arise after the groups have built up half of their final mass, due to merging of massive group members. We show that the existence of fossil systems is primarily driven by the relatively early infall of massive satellites, and that we do not find a strong environmental dependence for these systems. In addition, we find tentative evidence for fossil group satellites falling in on orbits with typically lower angular momentum, which might lead to a more efficient merger on to the host. We find a population of groups at higher redshifts that go through a 'fossil phase': a stage where they show a large magnitude gap, which is terminated by renewed infall from their environment.

Key words: methods: *N*-body simulations – galaxies: clusters: general – galaxies: evolution – galaxies: formation – dark matter.

1 INTRODUCTION

Observations in the last decade revealed the existence of groups of galaxies containing extended X-ray-emitting hot gas with properties expected for poor clusters such as the Virgo cluster, but in the optical light completely dominated by a single luminous, giant elliptical galaxy (Ponman et al. 1994; Vikhlinin et al. 1999). The second brightest galaxy in these systems is more than a factor of 5 less luminous than the dominant elliptical. More specific, these systems are defined observationally as spatially extended X-ray sources with luminosities $L_{\mathrm{X,bol}} \geqslant 10^{42}\, h_{50}^{-2}\, \mathrm{erg\,s^{-1}}$. The optical counterparts are massive galaxy groups in a mass range of 10^{13}–$10^{14}\, h^{-1}\, \mathrm{M}_{\odot}$, with $\Delta m_{12} \geqslant 2$ mag, where Δm_{12} is the absolute *R*-band magnitude gap between the brightest and second brightest galaxies within $0.5R_{200}$ (Jones et al. 2003).

These systems are extremely interesting for several reasons. Although they have X-ray temperatures comparable to the Virgo cluster these systems show a galaxy luminosity function with a deficit of bright galaxies beyond the characteristic magnitude of the Schechter function M^* (D'Onghia & Lake 2004), whereas Virgo contains six M^* galaxies (Jones, Ponman & Forbes 2000). Therefore they have been interpreted as the final outcome of galaxy–galaxy mergers. Numerical simulations suggest that the luminous galaxies in a group will eventually merge to form a single giant elliptical galaxy (e.g. Barnes 1989). The merging time-scales for the brightest group members (with magnitudes $M \sim M^*$ or brighter) in compact groups are typically a few tenths of a Hubble time. Therefore, by the present-day several group galaxies have likely merged into the giant elliptical. Possible candidates for systems about to form a fossil group are high-redshift compact groups. For example, Rines, Finn & Vikhlinin (2007) and Mendes de Oliveira & Carrasco (2007) report massive compact groups at higher redshift that would results in such a large magnitude gap.

Outside of the high-density core of fossil groups, the cooling time for the intra-group medium is larger than a Hubble time; thus, while the luminous galaxies in some groups have had enough time to merge into a single object, the large-scale X-ray halo of the original groups should remain intact. This means that a merged group might appear today as an isolated elliptical galaxy with a group-like X-ray halo (Ponman & Bertram 1993). Hence these systems have been termed 'fossil' groups.

Recent observations indicate that these systems have an enhancement in both the X-ray luminosity L_{X} as well as temperature T_{X} compared to normal groups (Khosroshahi, Ponman & Jones 2007).

⋆E-mail: sbenda@aip.de
†Marie Curie Fellow.

Jones et al. (2000) have studied the central galaxy of fossil group RXJ 1340.6+4018 in detail and found no evidence for spectral features implying recent star formation, which indicates the last major merger occurred at least several Gyr ago. Since they have not had any recent major merger, this makes them an ideal class of relatively undisturbed virialized objects to study e.g. the quiescent evolution in groups, and would make them ideal targets for e.g. lensing studies to constrain dark matter density profiles.

These systems are not rare. With a number density of $(5 \times 10^{-7}$–$2 \times 10^{-6})\, h^3\,\mathrm{Mpc}^{-3}$, they constitute 10–20 per cent of all clusters and groups with an X-ray luminosity greater than $2.5 \times 10^{42}\, h^{-2}\,\mathrm{erg\,s}^{-1}$ (Vikhlinin et al. 1999; Romer et al. 2000; Jones et al. 2003; Santos, Mendes de Oliveira & Sodré 2007). The number density of fossil groups is comparable to that of brightest cluster galaxies (Jones et al. 2003). Thus they may be of considerable importance as the place of formation of a significant fraction of all giant ellipticals. Khosroshahi, Ponman & Jones (2006) find support for this scenario, although the isophotes in the central early type of fossil systems seem to be different compared to the typical boxy isophotes of the brightest cluster galaxies.

So far different approaches to model and measure the number density of fossil systems have been undertaken. Milosavljević et al. (2006) adopted an extended Press–Schechter approach to estimate 5–40 per cent for the expected fraction of fossil groups in a mass range of 10^{13}–$10^{14}\, h^{-1}\,\mathrm{M}_\odot$ and decreasing to 1–3 per cent for massive clusters. In the 2dFGRS 6.5 per cent of groups with masses between 10^{13}–$10^{14}\, h^{-1}\,\mathrm{M}_\odot$ are qualified to be fossil (van den Bosch et al. 2007) and more recently Yang, Mo & van den Bosch (2008) estimate 20–60 per cent of the total group to be fossil in their Sloan Digital Sky Survey (SDSS) sample with masses $\approx 10^{13}\, h^{-1}\,\mathrm{M}_\odot$. Using *N*-body simulations D'Onghia et al. (2007) estimate a fraction of 18 per cent of the simulated group to be fossil whereas Sales et al. (2007) from an analysis of the Millennium Simulation (Springel et al. 2005) find 8–10 per cent of fossil systems with mass $M_{\mathrm{group}} > 10^{13}\, h^{-1}\,\mathrm{M}_\odot$. The definition of a fossil system in simulations is not a trivial task. Dariush et al. (2007) provide several measurements of the fraction of fossil systems in its sample of simulated groups and discuss expected differences in fraction due to selection effects. The authors show that differences in selection criteria have a large impact on the measured abundances. Note that some of the observed systems seem to be fossil clusters rather than fossil groups (Cypriano, Mendes de Oliveira & Sodré 2006; Gastaldello et al. 2007; Zibetti et al., in preparation), i.e. galaxy clusters with the typical magnitude gap of 2 mag between the brightest and the second brightest cluster galaxy. Although different works quote different estimates of abundances of fossil systems, a general consensus has been slowly emerging: a significant fraction of groups is fossil. This fraction is expected to rise strongly with decreasing group mass (Milosavljević et al. 2006; Dariush et al. 2007; van den Bosch et al. 2007; Yang et al. 2008).

Most of the theoretical work on fossil groups focused on the predictions of the statistics of the magnitude gap in the luminosity function. The physical processes that lead to the formation of a mass or magnitude gap in these systems are still poorly understood. Early work suggest that fossil groups result from mergers of the largest galaxies within compact groups (Barnes 1989) and are due to early formation time (Gao et al. 2004; D'Onghia et al. 2005; Zentner et al. 2005; Wechsler et al. 2006; Dariush et al. 2007). However, it is not yet understood under which conditions mergers are so efficient that they produce such an extreme gap in magnitude.

There are a number of open questions which we want to address here. When do fossil groups typically form their magnitude gap? Are fossil systems early formed systems, are they more concentrated than other systems? Is there any connection between the typical properties of fossil systems and environmental effects? In particular, are fossil groups long-lasting systems, or does the group environment regulate its lifetime by infall of new massive structures? These questions are addressed using a high-resolution *N*-body simulation, in which we focus on massive groups in a mass range of 1×10^{13}–$5 \times 10^{13}\, h^{-1}\,\mathrm{M}_\odot$, which is similar to the mass of the archetype fossil group RXJ 1340.6+4018 (Jones et al. 2000) and allows for a statistical significant sample. In contrast to previous theoretical studies of fossil groups, we follow the accretion histories of individual satellites, which allows for a detailed study of their accretion histories and orbital properties. The answers should guide the interpretation of observational data sets especially by surveys like PANSTARRS combined with COSMOz that can search for fossil systems at higher redshift and provide a framework for understanding the formation of giant ellipticals within the current cosmology.

This paper is organized as follows. We describe the numerical simulation in Section 2.1 and the selection criterion of the sample of fossil groups in Section 2.2. In Section 3 we describe the fossil group properties we find, like number density, formation time, concentration and time of last major merger and discuss how they compare to current observational constraints. Section 4 investigates the properties of infalling satellite haloes, and the formation mechanisms leading to a large magnitude gap. Our main results are summarized in Section 5.

2 METHODS

We have selected our sample of fossil groups from a $80\, h^{-1}\,\mathrm{Mpc}$ dark matter only *N*-body simulation which is large enough to lead to a statistically meaningful sample. Since we are mainly interested in the dynamical properties of the massive group members, we focus on a dark matter simulation in this work.

2.1 Simulation

The initial conditions were generated for a *WMAP*3 cosmology with matter density $\Omega_{\mathrm{m}} = 0.24$, an linear mass variance on $8\, h^{-1}\,\mathrm{Mpc}$ scale $\sigma_8 = 0.76$, a dimensionless Hubble parameter $h = 0.73$ and a spectral index of primordial density perturbations $n = 0.96$ (Spergel et al. 2007). We used $N = 512^3$ dark matter particles, i.e. a particle mass of $2.5 \times 10^8\, h^{-1}\,\mathrm{M}_\odot$. Starting at redshift $z = 40$ we evolved the simulation until the presence with the MPI version of the Adaptive Refinement Tree (ART) code (Kravtsov, Klypin & Khokhlov 1997). The ART code enabled us to reach a force resolution of 1–3 kpc in the most refined regions, making sure our massive subhaloes do not suffer from overmerging (Klypin et al. 1999) inside of our group sized haloes.

We identified groups with a friend-of-friends (FOF) algorithm with a linking length of $l = 0.17$ d (chosen to correspond to a mean overdensity of roughly 330), with d the mean interparticle distance. The advantage is that it identifies groups of any shape. In a second step we identified the bound (sub)structures in the groups. To this end we used the bound density maximum (BDM) halo finder (Klypin et al. 1999). This algorithm identifies density maxima and removes unbound particles from the haloes. Therefore it is particularly suitable to identify subhaloes and their properties, like their circular velocity. Since the determination of subhalo masses in groups is uncertain we characterized them by their maximum circular velocity. The BDM halo with the highest circular velocity within the FOF group is considered the host group halo. We found 116 groups in

the mass range of 1×10^{13}–$5 \times 10^{13}\,h^{-1}\,\mathrm{M}_{\odot}$, corresponding to the massive end of galaxy groups. We calculated the mass accretion histories of the haloes using 130 time-steps of equal distance in the expansion parameter, $\Delta a = 0.006$. To this end we selected the 20 per cent of the most bound particles of haloes and compare them in eight consecutive time-steps. We uniquely associated a halo to its progenitor by considering halo pairs, which have the largest number of particles in common and do not differ by more than a factor of 5 in mass. The last criterion was included to avoid spurious misidentification by subhaloes with their host halo.

2.2 Selection of fossil groups

Fossil groups are selected on the basis of a measured magnitude gap between the brightest and the second brightest group member. In our simulation we can only identify the dark matter haloes which host the group galaxies. Currently methods are being developed in order to relate galaxy luminosities to dark matter haloes in a statistical way (e.g. Vale & Ostriker 2004; Yang et al. 2004; Cooray & Milosavljević 2005; Conroy, Wechsler & Kravtsov 2006). Here we follow this idea and associate luminosities to the (sub)haloes in the group. We assume simply that the most luminous galaxy is the central galaxy of the group host halo with circular velocity $v_{\mathrm{circ},1}$. Consequently, the halo with the second highest circular velocity $v_{\mathrm{circ},2}$ will host the second brightest group galaxy. Here the circular velocity v_{circ} is always taken at the maximum of the rotation curve.

To model the magnitude gap we adopt a similar approach as Milosavljević et al. (2006) where we relate the halo circular velocity to the luminosity of the central galaxy using an empirically measured mean R-band mass-to-light ratio (Cooray & Milosavljević 2005). Assuming a Sheth–Thormen (Sheth & Tormen 1999) mass distribution function for the dark matter haloes and a functional form as in equation (1), which expresses the halo mass in luminosity for the central galaxies, Cooray & Milosavljević (2005) fit the measured R-band luminosity function of Seljak et al. (2005). We convert our circular velocities to luminosities by the relation

$$L(M) = L_0 \left(\frac{M}{M_0}\right)^a \left[b + \left(\frac{M}{M_0}\right)^{cd}\right]^{-1/d} \qquad (1)$$

with $L_0 = 5.7 \times 10^9\,\mathrm{L}_{\odot}$, $M_0 = 2 \times 10^{11}\,\mathrm{M}_{\odot}$, $a = 4$, $b = 0.57$, $c = 3.78$, $d = 0.23$, where we substitute masses by circular velocities using the relation found by Bullock et al. (2001): $M/(h^{-1}\,\mathrm{M}_{\odot}) = 10^{\alpha}[v_{\mathrm{circ}}/(\mathrm{km\,s^{-1}})]^{\beta}$, with $\alpha = 4.3$ and $\beta = 3.4$.

Mass accretion on to haloes stops at the time when they become subhaloes of a more massive object like a group. After infall they start to lose matter due to tidal interactions. Since baryons tend to lie deeper in the potential well, they will be less prone to get tidally stripped. Therefore, the total luminosity is more likely to be related to the mass at infall (see e.g. Kravtsov, Gnedin & Klypin 2004). Following this idea we characterize the subhaloes of the groups by their masses and circular velocities *at infalling times* on to the group. The choice of relating luminosities to the circular velocities of haloes at infalling time has been motivated by recent successes in matching the data by modelling the two- and three-point correlation functions (Berrier et al. 2006; Conroy et al. 2006; Marin et al. 2008).

We consider fossil groups with masses between 1×10^{13} and $5 \times 10^{13}\,h^{-1}\,\mathrm{M}_{\odot}$ which would correspond to systems with $T \sim 1$ keV (Jones et al. 2000). Recent work from Dariush et al. (2007) points out biases in defining fossil systems from X-ray or optical selection criteria. According to the fig. 5 of Dariush et al. (2007) in the range of mass considered here, only 10 per cent of the groups defined fossil in optical band are expected to be strong X-ray emitters.

3 DISTRIBUTION AND PROPERTIES OF FOSSIL GROUPS

3.1 Abundance

In this section our main aim is to characterize the properties of the fossil groups of our group sample in order to guide the interpretation of future observational constraints. We begin by computing the abundance of fossil systems in our catalogue.

Assuming a magnitude gap of $\Delta m_{12} \geqslant 2$ (see dashed line in Fig. 1) 24 per cent of the groups of our catalogue are classified as fossil, corresponding to a number density of $5.5 \times 10^{-5}\,h^3\,\mathrm{Mpc}^{-3}$. This rate is higher than previous estimates based on N-body simulations (D'Onghia et al. 2007), semi-analytic models (Dariush et al. 2007; Sales et al. 2007), and observational estimates (Vikhlinin et al. 1999; Romer et al. 2000; Jones et al. 2003; Santos et al. 2007; van den Bosch et al. 2007), which all get a fraction of around 10 per cent for groups in the mass range considered here, although a recent study of the SDSS give a fossil fraction consistent with ours (Yang et al. 2008).

However, there are a number of caveats to be considered when comparing estimates from these different works. Up to now only 15 fossil groups are known with observed X-ray data. Hence, the inferred abundances present large uncertainties. We have selected our sample within a relatively narrow mass range, and the fraction of fossil systems in this range drops rapidly with increasing mass according to Milosavljević et al. (2006) and Dariush et al. (2007) estimates. Thus, a fair comparison is difficult.

An additional difficulty comes from the selection of the radius adopted to define fossil systems. Different authors use different definitions. In our work we adopt one virial radius R_{vir}, instead of $0.5R_{200}$ used by Jones et al. (2003) or $1\,h^{-1}$ Mpc (Sales et al. 2007). Consulting fig. 5 of Dariush et al. (2007) changing one virial radius to half will increase the abundance approximately by a factor of 2. Probably the fairest comparison can be made with the fraction of optical fossil groups reported in Yang et al. (2008), since their mass bin at $10^{13}\,h^{-1}\,\mathrm{M}_{\odot}$ is similar to ours, and their selection is based on the magnitude gap within one virial radius as we do. Our fraction of 24 per cent is in good agreement with their measured 18–60 per cent.

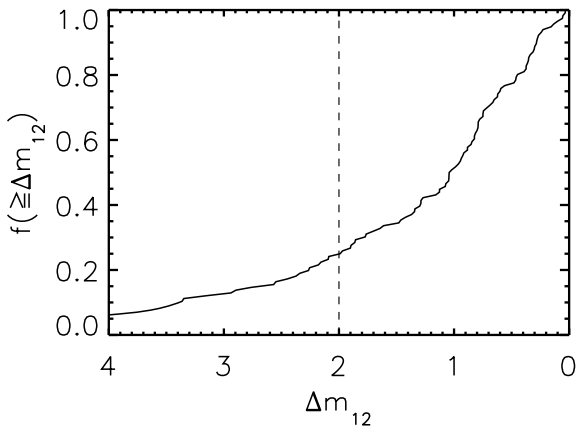

Figure 1. The fraction of galaxy-group-sized haloes with a magnitude gap parameter larger than Δm_{12}. The dashed line indicates our defining magnitude gap for fossil groups $\Delta m_{12} \geqslant 2$.

We note that some uncertainty comes from our adopted scheme for relating circular velocities to luminosities of the central galaxies in groups, where we followed Milosavljević et al. (2006) and Bullock et al. (2001). In this work, we are interested mainly in the formation process of systems with a large magnitude gap, which clearly corresponds to systems with a large gap in circular velocities even if the related magnitudes are uncertain. We therefore stick to our adopted method and study how our selected fossil population differs from the normal group population.

3.2 Environment density dependence

Fossil groups are systems with many properties typical for galaxy clusters. Hence, a further interesting test concerns the question whether fossil groups are isolated systems that populate the low-density regions or tend to reside in higher density regions of the Universe like galaxy clusters. A good test would be the cross-correlate the X-ray-emitting fossil groups with galaxies in the nearby Universe, e.g. with SDSS data (e.g. Santos et al. 2007). However, the limited number of fossil groups actually known makes an estimate of such correlations extremely difficult. Some observational indications, though still uncertain, would suggest that fossil groups could be fairly isolated systems (e.g. Jones, Ponman & Forbes 2000; Jones et al. 2003; Adami, Russeil & Durret 2007).

We check in our simulated sample of groups whether fossil systems populate preferentially low-density regions in the Universe. We estimate the environmental density on a scale of $4\,h^{-1}$ Mpc. To this end we determine the environmental overdensity $\Delta_4 = \rho_4/\rho_{\rm bg} - 1$, where ρ_4 is the dark matter density within $4\,h^{-1}$ Mpc from the group centre of mass, with the inner one virial radius subtracted, and $\rho_{\rm bg}$ is the background matter density. Our results are not affected by choosing a radius between 2 and $5\,h^{-1}$ Mpc. Fig. 2 shows the distribution of the overdensity Δ_4 for fossil and normal groups. Most of the groups, in the range of mass considered here, independent of being fossil or not, populate preferentially the intermediate overdensity region. A two-sided Kolmogorov–Smirnov test for the two cumulative distributions shown gives $D = 0.31$, corresponding to a probability of 0.03 that the two samples are drawn from the same distribution. We do not find a strong tendency for fossil systems to be preferentially located in low-density environments. We suggest therefore that observations might be biased to find fossil groups preferentially in low-density regions, which could be due to group selection effects.

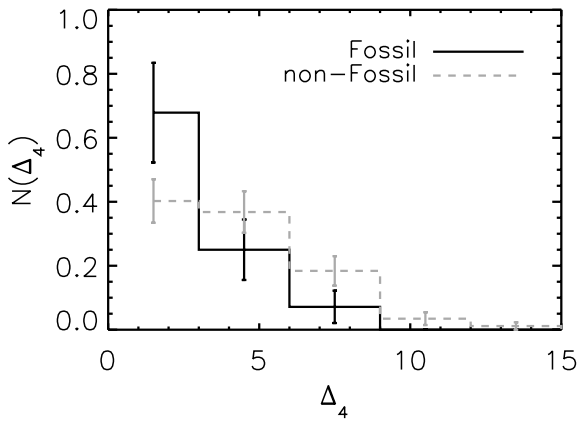

Figure 2. The group environment overdensity Δ_4 computed in a sphere of $4\,h^{-1}$ Mpc for fossil (black solid line) and non-fossil groups (grey dashed line). To compute the overdensity, the inner virial radius was subtracted. For comparison, cluster typically populate regions of $\Delta_4 > 10$. There does not seem to be a strong tendency for fossil groups to be in low-density environments. Error bars indicate 1σ Poissonian uncertainties.

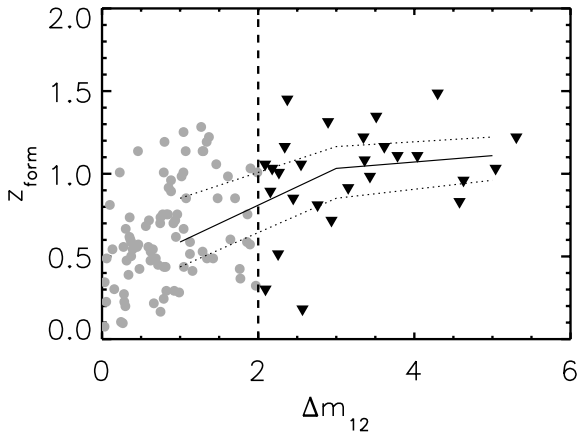

Figure 3. The correlation between the formation redshift of the group host halo and its magnitude gap parameter for fossil groups (triangles) and normal groups (circles). Overplotted are the mean values (solid line) and lower and upper quartiles (dotted lines).

3.3 Formation time

The halo formation redshift is defined as the epoch at which the system assembled 50 per cent of its final mass (e.g. Lacey & Cole 1993). Fig. 3 shows a correlation between the magnitude gap parameter and the formation redshift of the host halo for all the fossil systems (triangles) and the normal groups (grey circles). As pointed out in D'Onghia et al. (2005, 2007) and Dariush et al. (2007) this correlation shows that fossil groups form earlier than normal groups, albeit with large scatter. In order to assess this correlation we draw the mean and upper and lower quartiles (the solid and dotted lines in Fig. 2). The visual impression is quantified by statistical measures as the Pearson's linear correlation coefficient $r = 0.39$, implying a weak linear correlation between the magnitude gap and the formation time.

3.3.1 Concentration parameter

The early formation redshift is also reflected in a higher concentration parameter (Navarro, Frenk & White 1997).

We define the concentration of our haloes by the ratio of the virial radius of the host halo to the radius of a sphere enclosing one-fifth of its virial mass: $c_{1/5} = r_{\rm vir}/r_{1/5}$. This definition of the halo concentration allows for a robust concentration determination when the haloes are merger remnants and unrelaxed (Avila-Reese et al. 2005). The correlation shown in Fig. 4 between formation redshift and concentration is well fitted by a linear relation $z_{\rm form} = -0.79 + 0.27 \times c_{1/5}$ (marked with the dashed bold line).

The fossil groups clearly populate the early formed, more concentrated part of the plot, and have a mean concentration of $c_{1/5} = 6.4$, which is about 16 per cent higher than the concentrations found for normal groups $c_{1/5} = 5.5$. Our findings are consistent with fossil groups being systems with higher dark matter concentrations than usual groups, which supports such a trend found by Khosroshahi et al. (2007). At present there are yet few observational constraints on this issue (e.g. Gastaldello et al. 2007; Khosroshahi et al. 2007).

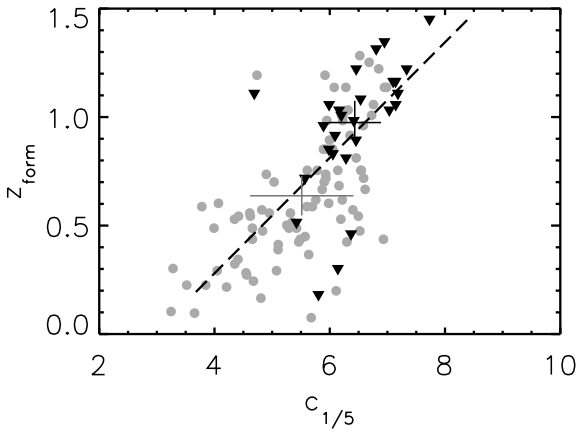

Figure 4. The formation redshift of the host halo as a function of the group concentration. The fossil group sample is marked with triangles and the normal groups are drawn with circles. The dashed line is a linear fit to all points. Crosses correspond to the mean values for the concentrations of fossil: $c_{1/5} = 6.4$ (bold cross) and non-fossil groups $c_{1/5} = 5.5$ (light cross), with the widths indicating the 1σ standard deviations.

However, upcoming X-ray observations of fossil groups with *Chandra* and *XMM* will provide better constraints soon.

3.4 Last major merger

Recent studies of the giant elliptical at the centre of fossil groups report no signs of a recent major merger activity, indicating that any major merger should have happened at least more than approximately 3 Gyr ago (Jones et al. 2000; Khosroshahi et al. 2006).

For each halo we estimate the time of the last major merger of the group haloes of our sample by studying the detailed mass assembly history. To identify the time of the last major merger, we denote a halo as a major merger remnant if its major progenitors were classified as a single group at one time but two separate groups with a mass ratio less than 4:1 at the preceding time. Note that when the mass ratio defining the major merger event is restricted to almost 1:1 progenitors, the time of the last major merger should in general coincide with the formation time (as defined above). We find that only 15 per cent of the fossil groups experienced the last major merger less than 2 Gyr ago, and at least 50 per cent had the last major merger longer than 6 Gyr in qualitative agreement with the observations.

4 FORMATION OF FOSSIL GROUPS

4.1 Forming the magnitude gap

We investigate the time evolution of the magnitude gap parameter of fossil systems in Fig. 5. The fossil groups are selected at $z = 0$ and the sample is traced backward in time to $z = 0.3$ (the right-hand top panel); $z = 0.65$ (the bottom panel on the left-hand side) and $z = 0.93$ (the bottom panel on the right-hand side). We find that the groups selected as fossil at present show a lower magnitude gap once traced backwards in time. They therefore do not qualify anymore as fossil systems at higher redshifts. The magnitude gap is typically formed over a wide range of redshifts between $z = 0$–0.7. It is worth noting that this happens typically after the group halo has gained half of its mass, which occurred earlier around redshift $z \geqslant 0.8$ (see Fig. 2). Similarly, Dariush et al. (2007) displays a set of snapshots ranging from $z = 0$ to 1 showing little infall of satellites at late times.

4.2 The fossil phase

Is the 'fossil stage' a final stage or will the systems fill their magnitude gap with the time? To assess this question, we select a sample of fossil systems at high redshift $z = 0.93$, and track these forward in time (as shown in Fig. 6). The open circles indicate massive fossil groups in the same mass regime as the sample selected at $z = 0$. Following all the fossil systems forward in time we note that they leave the range where they would be identified as fossil systems due to new infalling satellites. Only three of these systems did not experience further infall of a massive satellite from their surrounding environment so that they end up as a fossil system today.

Our simulation suggests that the existence of a gap in the galaxy luminosity function in fossil systems is only a transition phase in the evolution of groups, the duration of which is related to the merging of group members with the central object and infall of new haloes.

4.3 Properties of infalling satellites

We consider the population of infalling massive satellites to constrain their infalling time and orbital parameters.

First, we compute the average infalling rate of subhaloes falling into fossil systems as compared to normal groups. This quantity is computed by the cumulative number of massive (with $\Delta m_{12} \leqslant 2$) satellites falling into the host halo after redshift z divided by the total number of fossil (normal) groups: $\langle N_{\rm infall}(<z)\rangle = n_{\rm infall}(<z)/N_{\rm groups}$, which is plotted in Fig. 7 for fossil groups (black solid line) and non-fossil groups (grey solid line). Fig. 7 clearly shows that fossil groups accrete the larger satellites earlier in time as compared to the normal groups.

To ensure that this early infalling time is enough for the satellite to merge into the host, we give an estimate of the merger time due to dynamical friction. We adopt a fitting formula proposed by Jiang et al. (2008) in the form of

$$T_{\rm df} = \frac{0.94\epsilon^{0.60} + 0.60}{2C} \frac{m_{\rm pri}}{m_{\rm sat}} \frac{1}{\ln(1 + m_{\rm pri}/m_{\rm sat})} \frac{r_{\rm vir}}{V_{\rm circ}} \quad (2)$$

with $C = 0.43$, the orbit circularity parameter ϵ, the host virial radius $r_{\rm vir}$, circular velocity $V_{\rm circ}$, mass $m_{\rm pri}$ and the satellite mass $m_{\rm sat}$. This fitting function gives a good match to merger time-scales found in N-body simulations. We adopt the typical parameters for our groups of interest, $m_{\rm pri} = 10^{13}\,h^{-1}\,{\rm M}_\odot$, $r_{\rm vir} = 450\,h^{-1}$ kpc, $V_{\rm circ} = 350\,{\rm km\,s^{-1}}$ for the host, and $m_{\rm sat} = 10^{12}\,h^{-1}\,{\rm M}_\odot$. For the eccentricity we use $\epsilon = 0.4$, the peak of the eccentricity distribution measured by Jiang et al. (2008) and obtain a merger time-scale of $T_{\rm df} \approx 7.1$ Gyr, which is enough time for the massive satellites to merge into the host halo.

Note that for $z > 0.8$ fossil and non-fossil groups have similar infall history of massive satellites. In fact the slopes of the evolution of the infalling rate is the same for both distribution for $z > 0.8$, showing that the infalling rate of satellites is only different at low redshifts.

We checked whether the difference in infalling rate is determined by environment. This is done by splitting the sample up in $\Delta_4 < 5$ and $\Delta_4 \geqslant 5$ and evaluating the cumulative number of infalling satellites (see dashed lines in Fig. 7). Although the denser regions do experience a bit more infall, the difference is only of the order of 10–30 per cent, not as big as we observe for fossil and non-fossil systems (in agreement with Maulbetsch et al. (2007), who find little

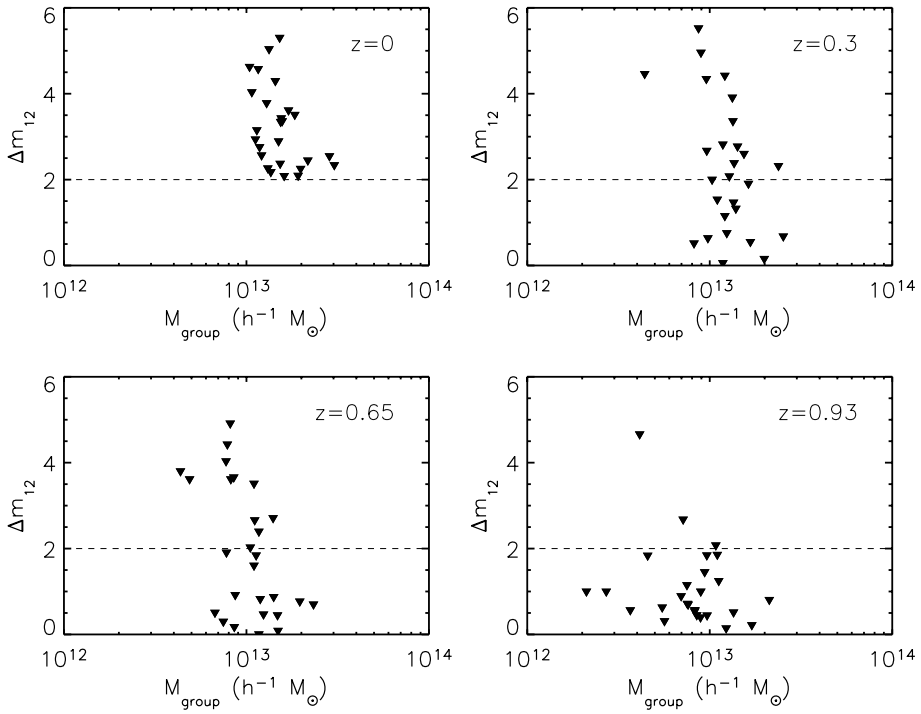

Figure 5. The evolution of the magnitude gap parameter Δm_{12} for fossil groups selected at $z = 0$ (for redshifts $z = 0$, 0.3, 0.65 and 0.93). The non-fossil groups, which constitute the majority of the groups, are left out from this plot for clarity. The plot shows that the majority of the fossil systems had one or more massive satellites at higher redshift. Note that the formation of the magnitude gap happens typically later (between $z = 0$ and 0.7) than the formation of the groups, which occurred around $z \geqslant 0.8$ (see Fig. 2).

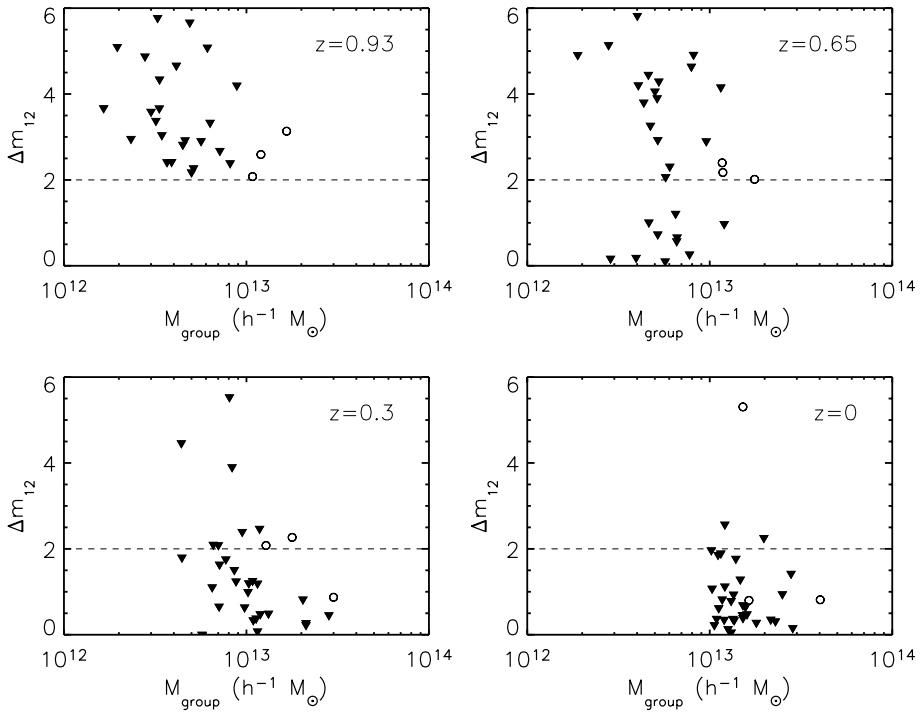

Figure 6. The evolution of the magnitude gap parameter Δm_{12} for fossil groups selected at $z = 0.93$ that end up in the $z = 0$ group sample, given at different epochs ($z = 0.93$, 0.65, 0.3 and 0). Again for clarity, only the selected sample at $z = 0.93$ is shown. The open circles indicate fossil groups that are selected in the same mass range as the group sample at $z = 0$. Most of the high-redshift fossil systems, when traced forward in time, experience renewed infall of massive satellites and become normal groups at $z = 0$. These systems are undergoing a 'fossil phase'.

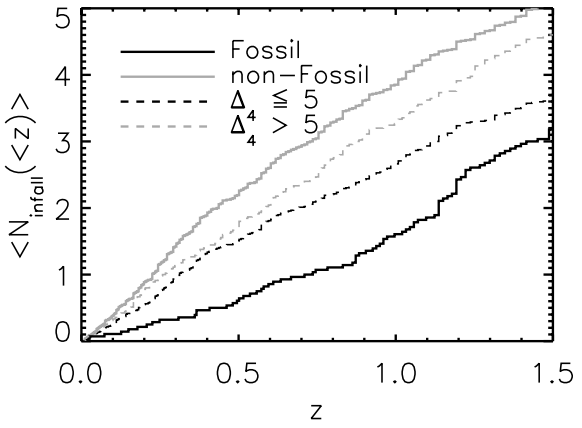

Figure 7. The mean cumulative number of massive satellites with $\Delta m_{12} < 2$ mag falling into the host halo at redshifts $z_{\rm infall} < z$. The grey solid line corresponds to normal groups and the black solid line to fossil groups. The dashed curves indicate the mean cumulative number of massive satellites when the group samples are split up by low dense regions $\Delta_4 \leqslant 5$ and higher dense regions $\Delta_4 > 5$.

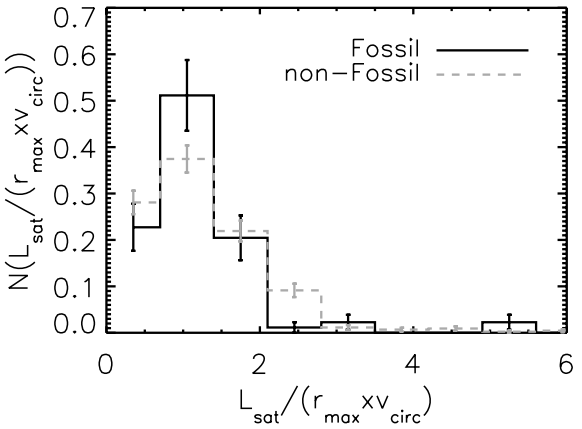

Figure 8. The distribution of the infalling satellite normalized angular momentum for fossil (black solid line) and non-fossil groups (grey dashed line). The distribution seems more narrowly distributed around $L_{\rm sat} \approx r_{\rm max} v_{\rm circ}$ for fossil groups, i.e. its high angular momentum tail seems to be less pronounced. Error bars indicate 1σ Poissonian uncertainties.

environmental dependence of the mass accretion history in this mass range). This supports lack of a strong environmental preference for fossil groups found in Section 3.2.

We address the question whether the conditions under which the massive satellites enter the group enable an efficient merger which could lead to a gap in the magnitude distribution of the fossil group galaxies. We checked the angular momenta values of the satellites at time of infall. Fig. 8 shows the angular momentum of the satellites at infalling time. The angular momentum is calculated by taking the cross product of the distance at infall and the velocity at infall $L_{\rm sat} = (\boldsymbol{r}_{\rm inf} \times \boldsymbol{v}_{\rm inf})/(r_{\rm max} v_{\rm circ})$, with $r_{\rm max}$ and $v_{\rm circ}$ both measured at the maximum of the rotation curve. Both distributions peak at $L_{\rm sat} \approx r_{\rm max} v_{\rm circ}$. Fossil groups seem to be lacking satellites in the high-end tail of angular momentum distribution, which may cause a faster merging of the satellites. However, since the distribution is rather poorly sampled, better number statistics are needed to confirm this result.

5 SUMMARY AND CONCLUSIONS

From an *N*-body simulation, we select and analyse a large sample of galaxy-group-sized haloes, that allows us to study in detail the mechanisms that lead to the formation of fossil systems in the hierarchical universe.

Our criterion to select fossil systems is based on identifying galaxy-group-sized haloes showing a gap in the magnitude between the two most massive members. This selection criterion assumes that the circular velocity of a halo traces its luminosity until it becomes a substructure of another more massive system. We relate the magnitude of our haloes to the circular velocities by using the empirical mean relation between dark matter halo mass and central galaxy *R*-band luminosity found by Cooray & Milosavljević (2005).

Our results may be summarized as follows.

(i) In the mass range 1×10^{13}–$5 \times 10^{13}\,h^{-1}\,{\rm M}_{\odot}$ 28 of the 116 groups sized haloes, i.e. 24 per cent qualify as fossil groups according to the definition of a magnitude gap of 2 mag between the brightest and second most bright galaxy. This fraction is higher than measured values. However, a fair comparison to observations is difficult, since differences due to varying selection criteria are expected. In addition, some uncertainty is expected in how to relate the mass or circular velocity of the haloes to the luminosities of their central galaxies. Because our adopted method of relating mass to galaxy luminosity is uncertain due to the broad scatter in this relation (Cooray 2006), and the rate is sensitive to the group definition, as well as selection effects, a robust comparison to observed number densities obtained by other authors is difficult at the moment. We are selecting systems with large circular velocity gaps or, respectively, mass gaps, so that our sample can be used to study the formation of the extreme magnitude gaps observed in fossil systems.

(ii) The fossil groups identified in our sample tend to form earlier than the other groups. This is in agreement with findings by Gao et al. (2004) and Zentner et al. (2005) who find a trend for systems with less substructure to form earlier. The fossil systems have assembled half of their final mass around $z \geqslant 0.8$ in agreement with the previous works. They form their magnitude gap typically between redshift $z = 0$–0.7, much later than the formation time of the groups. The early formation time is also expressed in a slightly higher dark matter concentration. The average concentration for the fossil groups is $c = 6.4$ compared to $c = 5.5$ of normal groups. Further, we find that the majority of the fossil group seem to have experienced the last major merger longer than 3 Gyr ago.

(iii) We do not find a strong correlation between the environment and the formation of fossil systems. Observations that indicate that fossil systems are found preferentially in low-density environments might be biased by selection effects.

(iv) The primary driver for the large magnitude gap is the early infall of massive satellites that is related to the early formation time of these systems. The difference in infalling rate for different group environments is only of the order of 10–30 per cent, far less than the observed difference between fossil and non-fossil groups, and hence the current environment does not seem the primary driver for the lack of massive satellites. This is in agreement also with the lack of strong correlation between fossil systems and environment.

(v) We suggest that efficient mergers of massive members within the groups can create the magnitude gap typical of fossil groups at any redshift. The efficiency of the merger process seems to be linked to the lower angular momentum of the massive satellites falling into the host halo of fossil groups when compared to normal groups. However, due to the limited number statistics we need more data to substantiate this.

(vi) By selecting samples of fossil groups at higher redshift ($z \approx 1$) we find that many of them do not exhibit the magnitude gap anymore once they are traced forwards until present time. The majority of them fill the magnitude gap with time by infall of new massive satellites. We conclude that the stage for a group to be 'fossil' is a transient phase.

ACKNOWLEDGMENTS

The computer simulation was done at Columbia supercomputer at NASA Ames Research Centre. AMvB-B acknowledges support from Deutsche Forschungsgemeinschaft (DFG) under the project MU 1020/6-3 and MU 1020/6-4. ED is supported by an EU Marie Curie Intra-European Fellowship under contract MEIF-041569. AK acknowledges support of NSF grant AST-04070702. MH acknowledges support from the DFG under the project Vo 855/2.

REFERENCES

Adami C., Russeil D., Durret F., 2007, A&A, 467, 459
Avila-Reese V., Colín P., Gottlöber S., Firmani C., Maulbetsch C., 2005, ApJ, 634, 51
Barnes J. E., 1989, Nat, 338, 123
Berrier J. C., Bullock J. S., Barton E. J., Guenther H. D., Zentner A. R., Wechsler R. H., 2006, ApJ, 652, 56
Bullock J. S., Kolatt T. S., Sigad Y., Somerville R. S., Kravtsov A. V., Klypin A. A., Primack J. R., Dekel A., 2001, MNRAS, 321, 559
Conroy C., Wechsler R. H., Kravtsov A. V., 2006, ApJ, 647, 201
Cooray A., 2006, MNRAS, 365, 842
Cooray A., Milosavljević M., 2005, ApJ, 627, L89
Cypriano E. S., Mendes de Oliveira C. L., Sodré L. J., 2006, AJ, 132, 514
Dariush A., Khosroshahi H. G., Ponman T. J., Pearce F., Raychaudhury S., Hartley W., 2007, MNRAS, 382, 433
D'Onghia E., Lake G., 2004, ApJ, 612, 628
D'Onghia E., Sommer-Larsen J., Romeo A. D., Burkert A., Pedersen K., Portinari L., Rasmussen J., 2005, ApJ, 630, L109
D'Onghia E., Maccio' A. V., Lake G., Stadel J., Moore B., 2007, MNRAS, submitted (arXiv:0704.2604)
Gao L., White S. D. M., Jenkins A., Stoehr F., Springel V., 2004, MNRAS, 355, 819
Gastaldello F., Buote D. A., Humphrey P. J., Zappacosta L., Seigar M. S., Barth A. J., Brighenti F., Mathews W. G., 2007, ApJ, 662, 923
Jiang C. Y., Jing Y. P., Faltenbacher A., Lin W. P., Li C., 2008, ApJ, 675, 1095
Jones L. R., Ponman T. J., Forbes D. A., 2000, MNRAS, 312, 139
Jones L. R., Ponman T. J., Horton A., Babul A., Ebeling H., Burke D. J., 2003, MNRAS, 343, 627
Khosroshahi H. G., Ponman T. J., Jones L. R., 2006, MNRAS, 372, L68
Khosroshahi H. G., Ponman T. J., Jones L. R., 2007, MNRAS, 377, 595
Klypin A., Gottlöber S., Kravtsov A. V., Khokhlov A. M., 1999, ApJ, 516, 530
Kravtsov A. V., Klypin A. A., Khokhlov A. M., 1997, ApJS, 111, 73
Kravtsov A. V., Gnedin O. Y., Klypin A. A., 2004, ApJ, 609, 482
Lacey C., Cole S., 1993, MNRAS, 262, 627
Marin F., Wechsler R., Frieman J., Nichol R., 2008, ApJ, 672, 849
Maulbetsch C., Avila-Reese V., Colín P., Gottlöber S., Khalatyan A., Steinmetz M., 2007, ApJ, 654, 53
Mendes de Oliveira C. L., Carrasco E. R., 2007, ApJ, 670, L93
Milosavljević M., Miller C. J., Furlanetto S. R., Cooray A., 2006, ApJ, 637, L9
Navarro J. F., Frenk C. S., White S. D. M., 1997, ApJ, 490, 493
Ponman T. J., Bertram D., 1993, Nat, 363, 51
Ponman T. J., Allan D. J., Jones L. R., Merrifield M., McHardy I. M., Lehto H. J., Luppino G. A., 1994, Nat, 369, 462
Rines K., Finn R., Vikhlinin A., 2007, ApJ, 665, L9
Romer A. K. et al., 2000, ApJS, 126, 209
Sales L. V., Navarro J. F., Lambas D. G., White S. D. M., Croton D. J., 2007, MNRAS, 382, 1901
Santos W. A., Mendes de Oliveira C., Sodré L. J., 2007, AJ, 134, 1551
Seljak U. et al., 2005, Phys. Rev. D, 71, 043511
Sheth R. K., Tormen G., 1999, MNRAS, 308, 119
Spergel D. N. et al., 2007, ApJS, 170, 377
Springel V. et al., 2005, Nat, 435, 629
Vale A., Ostriker J. P., 2004, MNRAS, 353, 189
van den Bosch F. C. et al., 2007, MNRAS, 376, 841
Vikhlinin A., McNamara B. R., Hornstrup A., Quintana H., Forman W., Jones C., Way M., 1999, ApJ, 520, L1
Wechsler R. H., Zentner A. R., Bullock J. S., Kravtsov A. V., Allgood B., 2006, ApJ, 652, 71
Yang X., Mo H. J., Jing Y. P., van den Bosch F. C., Chu Y., 2004, MNRAS, 350, 1153
Yang X., Mo H. J., van den Bosch F. C., 2008, ApJ, 676, 248
Zentner A. R., Berlind A. A., Bullock J. S., Kravtsov A. V., Wechsler R. H., 2005, ApJ, 624, 505

This paper has been typeset from a TEX/LATEX file prepared by the author.